Isotropic and anisotropic ^{13}C Knight shifts in the organic conductor DMTM(TCNQ)$_2$: NMR evidence for an interstack charge transfer at the inverted Peierls transition

G. Zimmer, A. C. Kolbert,* and M. Mehring
2. Physikalisches Institut, Universität Stuttgart, Germany

F. Rachdi and P. Bernier
Groupe de Dynamique des Phases Condensées, Université des Sciences et Techniques de Languedoc, 34095 Montpellier, France

M. Almeida
Dep. Quimica, National Laboratory for Engineering and Industrial Technology, 2686 Sacavem Codex, Portugal
(Received 19 December 1991; revised manuscript received 10 June 1992)

^{13}C NMR experiments on a single crystal of the organic conductor *N,N*-dimethyl-thiomorpholinium bis-tetracyanoquino-dimethane [DMTM(TCNQ)$_2$] are reported. The crystal was isotopically enriched at the C1 position of the TCNQ entity. Rotations about three orthogonal axes were performed, above and below the structural phase transition at 272 K, yielding the complete Knight-shift tensors and their relative orientations. Four isotropic shifts were observed, above T_c, with the number of isotropic resonances doubling below. The angular dependence of the resonance positions has allowed the correlation of half of the lines with each other, below T_c, as belonging to one of the two inequivalent stacks, with the other half being correlated with the other stack. Further, the resonances associated with one stack have been assigned to relative positions on the same molecule. The average coupling constant of the resonances assigned to each stack has yielded a relative charge distribution of 0.62 to 0.38 between the two stacks, below T_c.

I. INTRODUCTION

A. Organic conductor DMTM(TCNQ)$_2$

The organic conductor *N,N*-dimethyl-thiomorpholinium bis-tetracyanoquino-dimethane, DMTM(TCNQ)$_2$ has been the subject of considerable current interest largely due to its unusual first-order phase transition with $T_c=272$ K.[1-7] Upon *cooling* through T_c DMTM(TCNQ)$_2$ changes from a semiconducting state with $E_a=0.25$ eV to a state with a nearly temperature-independent conductivity, almost 3 orders of magnitude higher, along the stacking axis.[3] This behavior is opposite to that normally observed in TCNQ salts and has been referred to as an "inverted Peierls" phase transition.[3]

The structural changes associated with this phase transition are only partly understood. X-ray diffraction has established that, above T_c, DMTM(TCNQ)$_2$ has a monoclinic unit cell (space group $P2_1/m$) with the DMTM cation located on a mirror plane between two sheets composed of dimerized, parallel TCNQ stacks, as illustrated in Fig. 1 together with the labeling of the carbon atoms as referred to in the text.[2,8] The presence of the asymmetric cation, DMTM, on a mirror plane, above T_c, implies that the DMTM's are disordered in this phase.[2,8] A second moment analysis of broadline ^1H nuclear magnetic resonance (NMR) spectra has found the disorder to be dynamic, involving conformational motions of the DMTM ring.[7] The axis of highest conductivity, the crystallographic **c** axis makes an angle of 34° with respect to the axis perpendicular to the plane of the TCNQ molecule.[2,8] The dimerized TCNQ molecules in a stack are related by inversion centers.[8] Below T_c the complete x-ray structure has not been determined, due to experimental difficulties,[2,8] however, some general features are known. The unit cell changes to triclinic (space group $P1$

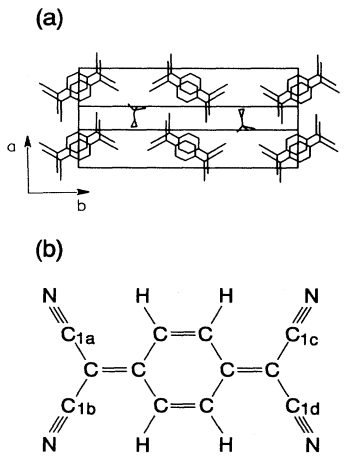

FIG. 1. (a) Schematic crystal structure (view along the **c** axis) of DMTM(TCNQ)$_2$ above T_c. (b) TCNQ with labeled carbon positions as referred to in the text.

or $P\bar{1}$) and the mirror plane is lost, probably due to DMTM ordering.[2,8] A phase transition involving cation ordering is known in $DMM(TCNQ)_2$, which is isomorphous to $DMTM(TCNQ)_2$, above T_c,[2,9] and the broadline ^1H NMR work confirms the loss of a motional degree of freedom of the DMTM cations below T_c.[7] The inversion centers between the TCNQ molecules are probably retained as the sheet structure does not change significantly at T_c.[8] This is confirmed by ^{13}C and ^1H magic-angle spinning NMR which show a doubling of the number of NMR lines below T_c, not a quadrupling, consistent with the loss of the mirror plane and the retention of the inversion centers.[5,7]

Recent NMR studies have also attempted to gain information on the electronic changes occurring at T_c via the measurement of ^{13}C and ^1H Knight shifts.[5,7] The measurement of locally resolved Knight shifts with high-resolution solid-state NMR has proven to be an important tool for the investigation of the electronic distribution in organic conductors,[10–15] in some cases yielding a complete spin-density map of the conduction-band orbital.[14,15] Previous high-resolution ^{13}C NMR on $DMTM(TCNQ)_2$ has involved the use of magic-angle spinning (MAS)[16,17] to measure isotropic Knight shifts of the TCNQ-C1 (cyano) carbons.[5] High-resolution ^1H NMR involving MAS and multiple pulse decoupling has been utilized to measure locally resolved ^1H Knight shifts, yielding the spin densities on the protonated (C4) carbons via the McConnell relation.[7] Making some assumptions regarding the assignment of the lines, an estimate of the charge distribution between the two inequivalent stacks below T_c was made in both of these studies. This represented an experimental indication for the interstack charge transfer proposed as a tentative explanation for the conductivity anomaly by Visser *et al.*[2]

In this paper we report the results of the temperature-dependent single-crystal study of $DMTM(TCNQ\text{-}1\text{-}^{13}C_4)_2$ which yielded the complete isotropic and anisotropic Knight shift of the C1 carbons, above and below the phase transition. Furthermore, we have used the angular dependence of the resonance positions to assign the lines and to confirm therefore the NMR evidence of the interstack charge transfer at T_c.

B. Knight shifts

The actual nuclear resonance frequency is always shifted away from the Larmor frequency $\omega_0=\gamma B_0$. In diamagnetic solids this shift is due to the shielding of the static magnetic field by the surrounding electrons and is called a chemical shift as it is strongly dependent on the local chemical environment. In conducting materials there is an additional shift, due to the averaged hyperfine coupling to the conduction electrons called the Knight shift.[18] As with the chemical shift, the Knight shift is generally a tensor quantity and is related to the hyperfine tensor through

$$\underline{K}=\frac{\chi_s}{\hbar\gamma_e\gamma_n}\underline{A} \tag{1}$$

in which χ_s is the spin susceptibility per conduction electron and γ_e and γ_n are the gyromagnetic ratios of the electron and nucleus, respectively. The hyperfine coupling tensor, $\underline{A}$, describes the interactions of the conduction electrons with the nucleus including Fermi contact, dipolar interactions, and core-polarization effects.

In metals this shift is due to the rapid motion of the conduction electrons at the Fermi surface with the Fermi velocity. Large paramagnetic shifts have been observed, however, in one-dimensional conductors with conductivities as low as 10^{-6} S/cm.[19] The presence of averaged hyperfine couplings, in view of the limited charge mobility in these systems, is an indication of rapid spin motion due to strong electron-electron couplings. As the rapid spin motion, even in the absence of charge mobility, is sufficient for averaged hyerfine couplings, and as the distinction between the two cases in practice is not always clear, we will continue to refer to all such shifts as Knight shifts.

The total shift Hamiltonian in the laboratory frame may be written as

$$H=-\gamma_n\hbar I\underline{\delta}B_0 \tag{2}$$

in which $\underline{\delta}$ is the total shift tensor and is given by

$$\underline{\delta}=\underline{K}+\underline{\sigma}\ , \tag{3}$$

where $\underline{K}$ and $\underline{\sigma}$ are the Knight- and chemical-shift tensors, respectively.[20] In the high-field limit, this equation is truncated, retaining only terms which commute with the Zeeman Hamiltonian, quantized along B_0, typically taken to be the z axis in the laboratory frame. For a rotation about an axis perpendicular to B_0, δ_{zz}, which is proportional to the eigenfrequencies of the Hamiltonian of Eq. (2), is in the laboratory frame, L, given by

$$\delta_{zz}=A+B\cos2\phi+C\sin2\phi\ , \tag{4}$$

in which ϕ is the angle relating a frame fixed on the goniometer, G, to L. Rotations of the crystal from $\phi=0$ to $\phi=\pi$ for three orthogonal orientations of the crystal frame, C, with respect to G will give nine parameters from the fits of Eq. (4) to the data, which can be used to determine the sum tensor, $\underline{\delta}_C$, in the crystal fixed frame. As $\underline{\delta}_C$ is symmetric, only six of the nine components are independent, providing an internal check for the consistency of the data. Determination of the Euler angles, $\Omega^{\delta}_{PC}=(\alpha_{PC},\beta_{PC},\gamma_{PC})$, relating $\underline{\delta}_C$ to $\underline{\delta}_P$, the sum tensor in its principal axis system (PAS), i.e., frame P, may be simply accomplished by determining the transformation $R(\Omega^{\delta}_{PC})$ which diagonalizes $\underline{\delta}_C$. For completeness, we note that the case of a powder, spinning at the magic angle, is described by the transformation to $\underline{\delta}_L$ via $R(\Omega^{\delta}_{RC})$ and $R(\Omega^{\delta}_{LR})$ transformations from frame C to a rotor fixed frame, R, in which the Ω^{δ}_{RC} are random, and a transformation from R to L, in which $\alpha_{LR}=\omega_r t$, $\beta_{LR}=\arctan\sqrt{2}$, and γ_{LR} is arbitrary. These transformations are discussed in detail in Ref. 21.

In order to obtain Knight-shift tensor information, one has to separate the chemical and Knight-shift contributions from the sum tensor. Experimentally several approaches have been used. Since the Knight shift is direct-

ly proportional to the spin susceptibility, χ_s, this has been exploited in two ways. The first method is to directly reduce the spin susceptibility by saturating the electronic spin system via microwave irradiation.[22,23] Unfortunately, such experiments are extremely difficult to perform at the magnetic fields required for high-resolution ^{13}C NMR, as a high-power microwave source at $\nu \geq 100$ GHz is required. The second, more experimentally tractable approach is to perform variable temperature experiments over a range in which the susceptibility changes substantially.[24]

Ultimately, neither of these methods will give a complete experimental separation of the chemical and Knight shifts, and acquiring data over a limited range in χ_s and extrapolating to $\chi_s = 0$, to obtain the chemical shift, may lead to large errors. A third approach is to simply subtract the chemical shift tensor of a neutral reference compound (such as TCNQ for TCNQ salts), avoiding the errors due to extrapolations. This approach depends upon the chemical-shift tensor of the anionic or cationic molecule being identical to that of the neutral species, which has been shown to be quite a good assumption for other organic conductors.[10,15,22] The use of this method, in general, requires some geometric reasoning about the relative orientations of the Knight and chemical-shift tensors,[15] and may not always be possible where only MAS data is concerned. In a single-crystal study, more information is available, namely the Euler angles relating the PAS of the $\underline{\delta}_{Ci}$ tensors separately to the crystal fixed frame.

Using this information the Knight-shift tensor contribution to the sum tensor may be extracted. As a self-consistent verification of the results, measurements have been performed at several different temperatures to determine that the Knight-shift tensor elements thus extracted had a linear dependence on the spin susceptibility, and to determine the statistical variation of the extracted parameters.

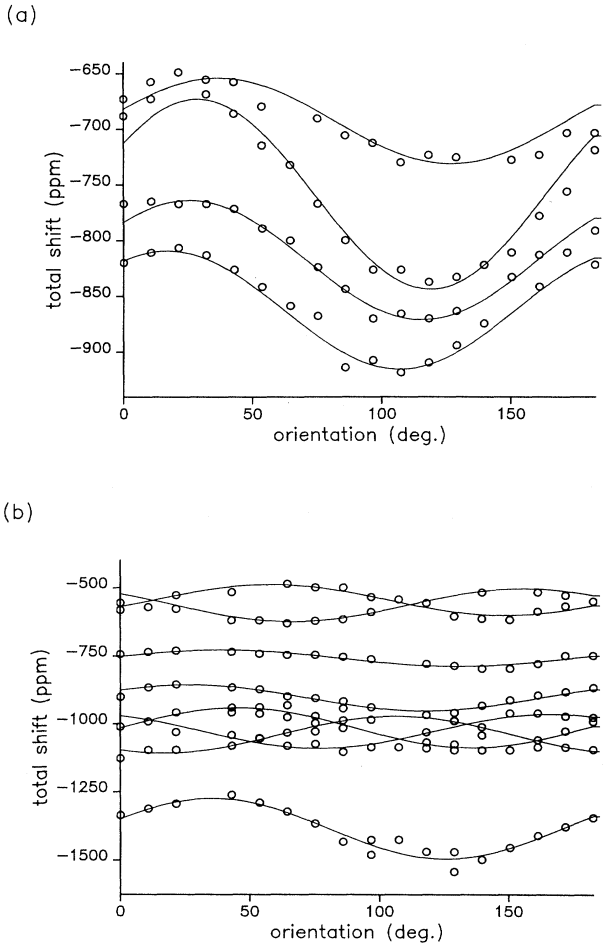

FIG. 2. Total frequency shift vs angle for a DMTM(TCNQ-1-$^{13}C_4)_2$ crystal rotating about an arbitrary axis, above and below T_c, at the temperatures indicated. (a) $T = 295$ K, (b) $T = 200$ K.

TABLE I. Knight shifts and hyperfine coupling constants for the C1 resonances in DMTM(TCNQ)$_2$. The first four lines are the resonances above the phase transition, the last eight are below. In both cases the lines are numbered in order of increasing shift from TMS (tetramethyl-silane). The Knight-shift tensors are reported for 295 K above T_c and 200 K below. The hyperfine tensors, below T_c, are the averages of the data taken at 140, 200, and 260 K. Average estimated errors are ± 0.5 MHz for the individual elements of $\underline{A}/2\pi$ and ± 0.4 MHz for $a_{iso}/2\pi$.

Line No.	K_{11}	K_{22}	K_{33}	K_{iso}	$a_{11}/2\pi$	$a_{22}/2\pi$	$a_{33}/2\pi$	$a_{iso}/2\pi$
		(ppm)				(MHz)		
1	−657	−825	−922	−801	−7.5	−9.4	−10.5	−9.1
2	−795	−878	−1002	−892	−9.1	−10.0	−11.4	−10.2
3	−842	−971	−1044	−952	−9.6	−11.1	−11.9	−10.9
4	−900	−1008	−1120	−1008	−10.3	−11.5	−12.8	−11.5
1	−584	−708	−727	−673	−5.3	−6.6	−7.2	−6.3
2	−575	−713	−773	−687	−5.5	−6.8	−7.4	−6.5
3	−793	−946	−984	−908	−7.3	−8.7	−9.6	−8.5
4	−973	−1050	−1154	−1059	−8.9	−9.7	−10.8	−9.8
5	−1058	−1225	−1303	−1195	−10.4	−11.0	−12.8	−11.4
6	−1241	−1249	−1308	−1266	−11.0	−11.5	−12.5	−11.6
7	−1401	−1440	−1586	−1476	−12.9	−13.4	−14.3	−13.5
8	−1462	−1537	−1572	−1524	−13.2	−14.0	−15.3	−14.1

II. RESULTS

Figure 2 shows the line positions versus angle for the rotation about the first of three orthogonal axes for a crystal DMTM(TCNQ-1-$^{13}C_4)_2$. Figure 2(a) was acquired above T_c ($T=295$ K) where there are clearly four resonances, while Fig. 2(b), acquired below T_c ($T=200$ K), exhibits eight lines. The solid curves are fits of Eq. (4) to the data. Complete rotation patterns were acquired at 295, 260, 200, and 140 K, and the data were treated as described above. The Knight shift and hyperfine coupling tensor data are summarized in Table I. The first check of the correctness of the data is illustrated by Fig. 3, which is a plot of the total isotropic shift, relative to TMS, versus susceptibility, with the temperatures given as an upper, nonlinear horizontal scale. The isotropic shifts correlate well with published isotropic shifts from MAS spectra, and a plot of the shift versus susceptibility gives a straight line, over the temperature range investigated.

III. DISCUSSION

A. Assignment of the resonances

For each resonance, i, at each temperature, the diagonalization of the sum tensor in the crystal frame, $\underline{\delta}_{Ci}$, gives a set of Euler angles $\Omega_{PC}^{\delta_i}$. The mapping of the $\underline{\delta}_{Ci}$ onto one another must reflect some aspect of the molecular or crystal geometry. In this manner, we have correlated lines on the same stack below T_c, and pairs of lines with related positions on the TCNQ molecule.

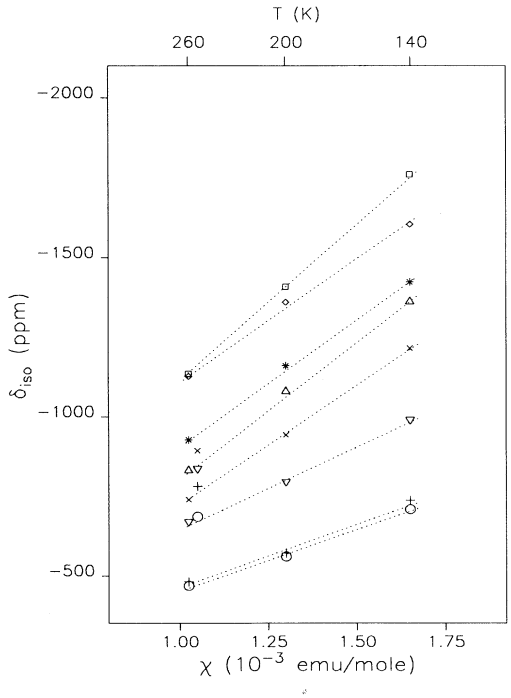

FIG. 3. Isotropic shifts ($\underline{\delta}_{iso}=\frac{1}{3}\,\mathrm{tr}\underline{\delta}$) vs susceptibility for a DMTM(TCNQ-1-$^{13}C_4)_2$ crystal. Shifts are relative to TMS.

For the C1 carbon, above T_c, the four $\underline{\delta}_{Ci}$ have one axis in common—the one oriented perpendicular to the molecular plane. Below T_c, this axis is parallel for the four C1 carbons on one of the two inequivalent stacks, and oriented about 68° with respect to the corresponding axes on the other stack. This allows the grouping of the lines on the same stack. Within the same stack, we can go one step further. The principal axis along the C≡N bond is parallel for cyano carbons related diagonally across the molecule, i.e., positions C_{1a}, C_{1d} and C_{1b}, C_{1c} in Fig. 1(b). Using this information we have determined lines 1 and 2 and lines 3 and 4, above T_c in Table I, to be related diagonally across the molecule, in this manner. Below T_c, lines 1–4 are correlated with one of the two inequivalent TCNQ stacks, we arbitrarily call stack A, while lines 5–8 belong to the other (stack B). Further lines 1 and 4, 2 and 3, 6 and 8, and 5 and 7, below T_c, are related diagonally, across the TCNQ molecule.

Using the isotropic hyperfine coupling constants from Table I, we can go one step further, with Coulombic arguments. Below T_c the spin density on the C1 carbons should be largerst for the cyano groups closest to the positive charge, which is localized on the nitrogen, of the ordered cation. This places lines 3 and 4 on stack A and lines 7 and 8 on stack B, on the side of the long TCNQ axis, closest to the nitrogen, to better compensate the charge. This of course assumes a very simple model for the dependence of the spin density on the isotropic hyperfine coupling constant, but it may be sufficient for the line assignment used here. The assignments are summarized in Fig. 4. Note that the left side of TCNQ (stack A) and the right side of TCNQ (stack B) is exposed to the uncharged (sulfer) end of the next DMTM ring as seen from the crystal structure of Fig. 1(a).

B. Separation of the chemical and Knight-shift tensors

As mentioned above, obtaining Knight-shift information from the sum tensor involves subtracting the contribution due to the chemical shift. The problem is that $\underline{K}_P$ and $\underline{\sigma}_P$ are related to the crystal frame by transformations involving Euler angles Ω_{CP}^{K} and Ω_{CP}^{σ}, which are in general different. Fortunately, we can derive a great deal of information about the orientation of the sum tensor in the molecular frame, using similar reasoning to that above, and for the rest we will rely on geometric arguments. Agreement of the Knight-shift principal axis system with that calculated via a model involving the dipo-

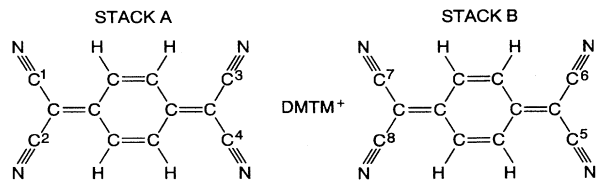

FIG. 4. Schematic projection of TCNQ stacks with assignment of the resonances below T_c, as labeled in Table I.

lar interaction of the conduction electrons in the p_z orbital with the nucleus has justified our arguments.

The chemical-shift tensor of the C1 carbons is axially symmetric with $\sigma_\perp = 211$ ppm and $\sigma_\parallel = -85$ ppm with $\sigma_\parallel$ oriented along the triple bond.[25] As discussed above, the sum tensor, $\underline{\delta}_{Ci}$, from each of the C1 resonances from a particular stack share one principal axis in common—the one perpendicular to the plane of the molecule along the p_z orbital. This is the principal axis of the intermediate value, which we designate δ_{33}. The axis along which the largest principal value δ_{11} lies is doubly degenerate, i.e., there are two possible orientations for the four tensors and they make an angle of $\sim 2\pi/3$ with respect to one another. The same holds for the axis of the smallest principal value, δ_{22}. If we assume that the largest value of $\underline{\delta}_P$ lies along the C≡N bond, we then have

$$K_{11} = \delta_{11} - \sigma_\parallel , \tag{5}$$

$$K_{22} = \delta_{22} - \sigma_\perp , \tag{6}$$

$$K_{33} = \delta_{33} - \sigma_\perp , \tag{7}$$

in which K_{11}, the smallest absolute value, lies along the C≡N bond, the intermediate value, K_{22}, lies perpendicular to K_{11}, but in the molecular plane, while K_{33}, the largest absolute value is perpendicular to the plane of the molecule, along the p_z orbital, as illustrated in Fig. 5. This orientation for $\underline{K}_P$ is consistent with the orientation obtained from the dipolar model, using theoretical spin densities, thus our assumption is justified.

C. Support for the interstack transfer model

The isotropic hyperfine coupling, derived from the isotropic Knight shifts, arises from the Fermi contact interaction between the electrons and the nuclei. As such they depend linearly on the spin density at the nuclear site, ρ. Deriving the π spin densities, ρ_π directly, however, is problematic as contributions from neighbors to ρ cannot be neglected. First note that the average isotropic hyperfine coupling does not change significantly at T_c. For the C1 carbon, from Table I above T_c, $\langle a_{iso} \rangle_{av}/2\pi = -10.4 \pm 0.4$ MHz, and below T_c $\langle a_{iso} \rangle_{av}/2\pi = -10.2 \pm 0.4$ MHz, confirming the constancy of the total spin density through T_c, i.e., there is no additional charge transfer at T_c, between TCNQ and DMTM, merely a redistribution on the stacks. This is consistent with recent ^1H NMR results which $\langle a_{iso} \rangle_{av}/2\pi = -2.0 \pm 0.1$ MHz above T_c and -1.9 ± 0.1 MHz below.[7] The mean value of the theoretical hyperfine coupling constant resulting from INDO (intermediate neglect of differential overlap) type MO (molecular orbital) calculations is -9.3 MHz due to a spindensity of -0.02 ($\rho_\pi = 0.0012$).

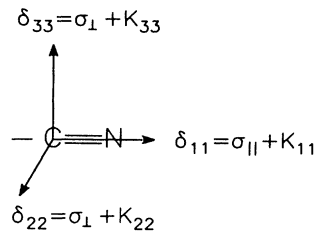

FIG. 5. Axis system describing the relative orientations of the Knight-shift tensor, $\underline{K}$, chemical shift tensor, $\underline{\sigma}$, and sum tensor, $\underline{\delta}$ of DMTM(TCNQ)$_2$.

Below T_c, averaging a_{iso} obtained from the lines assigned to each stack, we have $\langle a_{iso}(1-4) \rangle_{av}/2\pi = -7.8$ MHz and $\langle a_{iso}(5-8) \rangle_{av}/2\pi = -12.6$ MHz yielding a relative spin distribution between the two stacks of 0.62 to 0.38. These values correspond to those obtained from MAS results (0.62 to 0.38) (Ref. 5) and from multiple pulse ^1H measurements (0.65 to 0.35),[7] and represent an electron transfer at T_c of 24% of the spin density from one stack to the other, supporting the explanation for the conductivity anomaly proposed by Visser and others.[2,3]

IV. EXPERIMENT

99% enriched TCNQ-1-$^{13}C_4$ was synthesized from 1,4-cyclohexanedione and enriched malononitrile.[26] The enriched malononitrile was prepared from commercially available (Aldrich and CEA) sodium cyanide-^{13}C and bromoacetic-1-^{13}C to obtain TCNQ-1-$^{13}C_4$, respectively. Enriched DMTM(TCNQ)$_2$ was prepared by the reaction of the cation iodide with enriched TCNQ in boiling acetonitrile, using the same technique as previously described for the other TCNQ complex salts.[27,28] Due to the stresses induced in the crystal at the structural phase transition, care was taken not to cycle across T_c unnecesarily. The crystal needed to survive five passages through T_c, as the $\pi/2$ rotations necessary to obtain the initial orientations for the different rotations could only be done at room temperature, whereas the complete rotations at different temperatures were performed without warming up. All experiments were performed on a homebuilt pulse spectrometer operating at a ^{13}C frequency of 45.6 MHz. The probe was also homebuilt and was equipped with a single axis goiniometer allowing rotations of a 5-mm-diameter glass tube about an axis perpendicular to the static magnetic field. The single crystals with dimensions $\sim 0.2 \times 2 \times 4$ mm^3 were fixed in a Kel-F cube machined to fit tightly inside the glass tube, allowing accurate initial orientations for the orthogonal rotations. Estimated errors in the initial orientations are $\sim 5°$. Spectra were acquired after a single pulse at the ^{13}C frequency under ^1H decoupling at a field strength $\omega_1/2\pi \sim 50$ kHz. As the spin-lattice relaxation times are on the order of 10 ms, the average dissipated power was the rate limiting feature of the acquisition. Typical acquisition parameters were 1 ms of ^1H decoupling followed by a 100-ms recycle time, with 2000–5000 scans being averaged per spectrum.

V. CONCLUSIONS

We have performed ^{13}C single crystal measurements on DMTM(TCNQ-1-$^{13}C_4$)$_2$ above and below the structural phase transition at 272 K. The spectral lines resulting

from the stack below T_c, have been correlated with each other, and lines on one stack have been assigned to relative positions on the TCNQ molecule. The complete hyperfine coupling tensors have been determined and the isotropic parts have been used to calculate a relative charge distribution of 0.62 to 0.38 between the two inequivalent stacks below T_c. Agreement between these values and those obtained from ^{13}C MAS (Ref. 5) and high-resolution multiple pulse ^1H NMR (Ref. 7) is excellent. These results provide the first experimental evidence supporting the model of an interstack electron transfer at T_c, proposed by Visser *et al.*[2,3] to explain the conductivity anomaly.

ACKNOWLEDGMENTS

We acknowledge helpful advice on the synthesis of the labeled compounds from Dr. J. M. Fabre. This research was supported by the Deutsche Forschungsgemeinschaft under SFB 329. A. C. K. is supported by the NSF and NATO.

*Present address: Department of Chemistry, University of California, Berkeley CA 94720.

[1]S. Oostra, J. L. De Boer, and P. De Lange, J. Phys. (Paris) Colloq. **44**, C3-1387 (1983).

[2]R. J. J. Visser, S. Van Smaalen, J. L. De Boer and A. Vos, Mol. Cryst. Liq. Cryst. **120**, 167 (1985).

[3]M. Almeida, L. Alcacer, S. Oostra, and J. L. De Boer, Synth. Met. **19**, 445 (1987).

[4]F. Rachdi, M. Ribet, P. Bernier, and M. Almeida, Synth. Met. **35**, 47 (1990).

[5]F. Rachdi, T. Nunes, M. Ribet, P. Bernier, M. Helmle, M. Mehring, and M. Almeida, Phys. Rev. B **45**, 8134 (1992).

[6]G. Zimmer, A. C. Kolbert, F. Rachdi, P. Bernier, M. Almeida, and M. Mehring, Chem. Phys. Lett. **182**, 673 (1991).

[7]A. C. Kolbert, G. Zimmer, F. Rachdi, P. Bernier, M. Almeida, and M. Mehring, Phys. Rev. B **46**, 674 (1992).

[8]R. J. Visser, J. L. De Boer, and A. Vos, Acta Crystallogr. Sect. C **46**, 864 (1990).

[9]J. A. M. Middledorp, R. J. J. Visser, and J. L. De Boer, Acta Crystallogr. Sect. B **41**, 369 (1985).

[10]M. Mehring and J. Spengler, Phys. Rev. Lett. **53**, 2441 (1984).

[11]P. Bernier, M. Audenaert, R. J. Schweizer, P. C. Stein, D. Jerome, K. Bechgaard, and A. Moradpour, J. Phys. (Paris) Lett. **46**, L675 (1985).

[12]M. Mehring, M. Helmle, D. Köngeter, G. G. Maresch, and S. Demuth, Synth. Met. **14**, 349 (1987).

[13]J. Wieland, U. Haeberlen, D. Schweitzer, and H. J. Keller, Synth. Met. **19**, 393 (1987).

[14]D. Köngeter and M. Mehring, Phys. Rev. B **39**, 6361 (1989).

[15]T. Klutz, I. Hennig, U. Haeberlen, and D. Schweizer, J. Appl. Magn. Reson. **2**, 441 (1991).

[16]E. R. Andrew, A. Bradbury, and R. G. Eades, Nature (London) **182**, 1659 (1958).

[17]I. J. Lowe, Phys. Rev. Lett. **2**, 285 (1959).

[18]W. Knight, Solid State Phys. **2**, 93 (1956).

[19]A. C. Kolbert and M. Mehring, J. Magn. Reson. (to be published).

[20]A point of possible confusion arises here as to the sign conventions for the chemical and Knight shifts. This is due to the fact that chemical shifts to positive frequencies have historically been defined as negative, or down*field* shifts, while Knight shifts to positive frequencies have been defined as positive. In the study of synthetic metals, which exhibit both large chemical and Knight shifts, this may lead to problems, as the reported sign of a spectral shift then depends on its origin, which may not be *a priori* known. In this paper we have avoided the issue by defining positive frequency shifts as positive, regardless of their origin. This convention is reflected in the form of Eq. (3).

[21]M. Mehring, *High Resolution NMR in Solids* (Springer-Verlag, Berlin, 1983).

[22]W. Stöcklein, H. Seidel, D. Singel, R. D. Kendrick, and C. S. Yannoni, Chem. Phys. Lett. **141**, 277 (1987).

[23]R. A. Wind, H. Lock, and M. Mehring, Chem. Phys. Lett. **141**, 283 (1987).

[24]P. C. Stein, P. Bernier, and C. Lenoir, Phys. Rev. B **35**, 4389 (1987).

[25]T. Nunes, A. Vainrub, M. Ribet, F. Rachdi, P. Bernier, and M. Almeida, J. Chem. Phys. **96**, 8021 (1992).

[26]D. S. Acker and W. R. Hertler, J. Am. Chem. Soc. **84**, 3370 (1962).

[27]M. Almeida and L. Alcacer, J. Cryst. Growth **62**, 183 (1983).

[28]M. Almeida, L. Alcacer, and A. Lindegaard-Andersen, J. Cryst. Growth **72**, 567 (1985).